ISSN 0915-6364

# NATIONAL INSTITUTE FOR FUSION SCIENCE

An Extended Formula for the Energy Spectrum of Sputtered Atoms form a Material Irradiated by Light Ions

T. Ono, Y. Aoki, T. Kawamura, T. Kenmotsu, Y. Yamamura

(Received - Sep. 17, 2004 )

NIFS-DATA-89 Oct. 2004



TOKI, JAPAN

# An extended formula for the energy spectrum of sputtered atoms from a material irradiated by light ions*

T. Ono[a], Y. Aoki[a], T. Kawamura[b], T. Kenmotsu[c], Y.Yamamura [a+]

[a] *Okayama University of Science, 1-1 Ridai-cho, Okayama 700-0005, Japan*

[b] *Chubu University, 1200 Matsumoto-cho, Kasugai-shi, Aichi 487-8501, Japan*

[c] *Kibi International University, 8 Iga-cho, Takahashi-shi, Okayama 716-8508, Japan*

**Abstract**

We extend a formula proposed by Kenmotsu et al. (hereafter Paper I), which fits with the energy spectrum of atoms sputtered from a heavy material hit by low-energy light ions ($H^+$, $D^+$, $T^+$, $He^+$) by taking into account an inelastic energy loss neglected in Paper I. We assume that primary knock-on atoms produced by ions backscattered at large angles do not lose energy while penetrating the material up to the surface, instead of the energy-loss model used in Paper I. The extended formula is expressed in terms of a normalized energy-distribution function and is compared with the data calculated with the ACAT code for 50 eV, 100 eV and 1 keV $D^+$ ions impinging on a Fe target. Our formula fits well with the data in a wide range of incident energy.

**PACS:** 68.49.Sf, 52.40.Hf, 52.40.-W, 02.70.Uu

**Keywords:** Sputtering, erosion, Plasma-Materials interaction, First Wall Materials

---

[+]Deceased on 30th, March, 2004.

* A manuscript of a paper presented at 16th International Conference on Plasma Surface Interactions in Controlled Fusion Devices during May 24-28, 2004 in Portland, Maine, U.S.A..

## I. Introduction

The energy distribution function of atoms sputtered from the divertor plate and the first wall of a fusion device is indispensable in the analysis of the impurity transport in a scrape-off layer. The Thompson formula [1] has been used widely for this purpose. It assumes that sputtered atoms originate in a well-developed collision cascade created only by heavy ions in a material. However, an experiment [2] shows that the energy spectrum due to low-energy light ions differs from that calculated with the formula. This deviation can be understood from the fact that light ions cannot produce such a cascade, but rather a single or multiple collision sequence. Considering that an elastic energy loss is greater than an inelastic one for ions with energy of about a few hundred eV, we derived a formula for the energy spectrum of sputtered atoms due to light ions ($H^+$, $D^+$, $T^+$, $He^+$) by assuming that the primary knock-on atoms created near the surface with large-angle backscattered ions are the main candidates for ejection and by neglecting inelastic energy loss in Paper I [3]. In what follows, we derive an extended formula which can be applied to an energy region ranging from several tens of eV to keV, by considering both elastic and inelastic energy losses. We assume that primary knock-on atoms do not lose energy while penetrating a material up to the surface [4]. The extended formula is expressed in terms of a normalized energy distribution function and is compared with the data calculated with a Monte Carlo code ACAT [5], the Thompson and other formulas for 50 eV, 100 eV and 1 keV $D^+$ ions impinging on a Fe target.

## II. Model

In this paper, we treat sputtering of heavy materials with light ions with incident energy ranging from several tens of eV to a few keV. We use the same sputtering mechanism as in Paper I. We introduce a primary recoil density $F_p(E, E_0)$ in the way that $F_p(E, E_0)dE_0$ is the average number of primary recoil atoms created with energy $E_0$ in a collision cascade or sequence initiated by a light ion with initial energy $E$. For a collision between a light ion and a heavy target atom, from eqs.(1) and (2) of Paper I, the integral equation for $F_p(E, E_0)$ can be reduced to the following equation [3, 6]:

$$\int d\sigma(E,T)\left[T\frac{\partial}{\partial E}F_P(E,E_0)\right]+S_e(E)\frac{\partial}{\partial E}F_P(E,E_0)=\frac{d\sigma(E,E_0)}{dE_0}, \tag{1}$$

where $T$ is the energy of a recoil atom after a collision governed by a differential cross section $d\sigma$: $S_e(E)$ is an electronic stopping cross section: According to Lindhard et al. [7], $d\sigma$ is defined in reduced notation as

$$d\sigma=\frac{\pi a^2}{2}\frac{f(t^{1/2})}{t^{3/2}}dt, \tag{2}$$

with

$$t\equiv\varepsilon^2\frac{T}{T_{\max}}, \tag{3}$$

where

$$T_{\max}=\gamma E, \tag{4}$$

with $\gamma\equiv 4M_1M_2/(M_1+M_2)^2$: $M_1$ and $M_2$ are the masses of an incident ion and a target atom: $\varepsilon$ is the dimensionless reduced energy defined as

$$\varepsilon\equiv\left(\frac{a}{Z_1Z_2e^2}\right)\left(\frac{M_2E}{M_1+M_2}\right), \tag{5}$$

where $Z_1$ and $Z_2$ are their atomic numbers: $e$ is the unit charge: $a$ = 0.04685$(Z_1^{2/3} + Z_2^{2/3})^{-1/2}$ nm is the Thomas-Fermi screening length: $f(t^{1/2})$ is a scattering function defined by

$$f(t^{1/2})=\lambda t^{1/2-m}(1+(2\lambda t^{1-m})^q)^{-1/q}, \tag{6}$$

where $m$, $\lambda$ and $q$ are fitting variables for interatomic potentials. A data set of $(m, \lambda, q)$ = (0.25, 2.54, 0.475) was derived in the range $10^{-5} \leq t^{1/2} \leq 10$ [8]. We approximate the right-hand side of eq.(6) with above data set with an accuracy of 30 % by a simple function

$$f(t^{1/2})=\lambda_m t^{1/2-m}. \tag{7}$$

Then, we have $m$ = 1/4 and $\lambda_{1/4}$ = 2.54 for $10^{-5} \leq t^{1/2} \leq 1.18\text{x}10^{-2}$ referred to as region (I) and $m$ = 1/2 and $\lambda_{1/2}$ = 0.276 for $1.18\text{x}10^{-2} \leq t^{1/2} \leq 1.11$ referred to as region (II). Substituting eqs.(3) and (4) for eq.(2), one reaches

$$\mathrm{d}\sigma(E,T) = C_m E^{-m} T^{-1-m} \mathrm{d}T, \tag{8}$$

with $C_m = \pi\lambda_m a^2(M_1/M_2)^m(2Z_1Z_2e^2/a)^{2m}/2$. In the energy range concerned here, $S_e(E)$ is given as

$$S_e(E) = K_L E^{1/2}, \tag{9}$$

with $K_L = 1.216\text{x}10^{-2} Z_1^{7/6} Z_2 / M_1^{1/2} (Z_1^{2/3} + Z_2^{2/3})^{3/2}$ eV$^{1/2}$ nm$^2$ [9]. Substituting eqs.(8) and (9) for eq.(1) results in

$$\left[C_m E^{-m} \int_0^{T_1} T^{-m} \mathrm{d}T + K_L E^{1/2}\right] \frac{\partial}{\partial E} F_p(E,E_0) = C_m E^{-m} E_0^{-1-m}, \tag{10}$$

where $T_1$ is the maximum energy of a recoil atom transferred from a colliding atom. As cited above, an ion is backscattered at a large angle first by a target atom and then knocks off a target atom near the surface, mostly in the top layer, on its way out [10]. Thus, we set $T_1$ = $\gamma E_{back}$, where $E_{back}$ is the energy of a backscattered ion. $E_{back}$ varies with the position of an ion, since it loses energy while moving along its trajectory in a material. However, in this work, we set $E_{back} = (1-\gamma)E_{inc}$ for simplicity, where $E_{inc}$ is the incident energy of an ion. Then, we finally take $T_1 = \gamma\,(1-\gamma)E_{inc}$. By setting $E = E_{back}$ in eqs.(4) and (5), from eq.(3), the regions (I) and (II) for $f(t^{1/2})$ are reduced to (I) $10^{-5} \leq \varepsilon\, T^{1/2}/T_{max}^{1/2} \leq 1.18\text{x}10^{-2}$ and $1.18\text{x}10^{-2} \leq \varepsilon\, T^{1/2}/T_{max}^{1/2} \leq 1.11$ for a collision between a backscattered ion and a target atom. Then, from eq.(10), one obtains

$$\frac{\partial F_p(E,E_0)}{\partial E} = A E_0^{-5/4} E^{-3/4}, \tag{11-I}$$

where $A = C_{1/4}/(4C_{1/4}(\gamma\,(1-\gamma))^{3/4}/3 + K_L)$ with $C_{1/4} = \pi\lambda_{1/4}a^2(M_1/M_2)^{1/4}(2Z_1Z_2e^2/a)^{1/2}/2$ for region (I), and

$$\frac{\partial F_p(E,E_0)}{\partial E} = \frac{C_{1/2} E_0^{-3/2} E^{-1/2}}{2C_{1/2}(\gamma(1-\gamma))^{1/2} + K_L E^{1/2}}, \qquad (11-\text{II})$$

with $C_{1/2} = \pi\lambda_{1/2} a^2 (M_1/M_2)^{1/2} (2Z_1Z_2e^2/a)/2$ for region (II). In obtaining eq.(11), the lower limit of the integration over $T$ is extended to zero for simplicity, which, however, does not influence the result. In deriving eq.(11-II), we ignore the integration value in region (I), since it is smaller than that in region (II). Since the second term becomes larger than the first one in the denominator of eq.(11-II) for $\varepsilon\, T^{1/2}/T_{max}^{1/2} \geq 1.11$ and since $f(t^{1/2})$ given by eq.(6) with the above data set decreases sharply there, we can use the right-hand side of eq.(11-II) for approximation to $\partial F_p(E,E_0)/\partial E$ even beyond the upper limit of region (II). The lower limit of the integral of the derivative (11), $E_{min}$, is the minimum energy of a backscattered ion. We use the same physical hypothesis in estimating $E_0$ from $E_{min}$ as that employed above to calculate $T_1$ from $E_{inc}$, i.e., $\gamma\,(1-\gamma)E_{min} = E_0$. Thus, we can set $E_{min} = E_0/\gamma\,(1-\gamma)$. The upper limit of the integration over $E$ is clearly $E_{inc}$. From a physical reason for $F_p(E,E_0)$, it is clear that $F_p(E,E_0) = 0$ for $E_0 \geq E$. Under this condition, we can obtain $F_p(E,E_0)$ by integrating eq.(11) for regions (I) and (II).

The double differential sputtering yield is expressed as [4]

$$J(E_1,\boldsymbol{e}_1) = \int_U^{\gamma(1-\gamma)E_{inc}} \mathrm{d}E_0 \int_0^{\infty} \mathrm{d}x \int \mathrm{d}^2\boldsymbol{e}_0\, \hat{F}(E_{inc},\boldsymbol{e};E_0,\boldsymbol{e}_0,x)\, P(E_0,\boldsymbol{e}_0,x;E_1,\boldsymbol{e}_1), \qquad (12)$$

where $E_1$ and $\boldsymbol{e}_1$ are the energy and the direction of a sputtered atom: $\hat{F}\,\mathrm{d}x\mathrm{d}E_0\mathrm{d}^2\boldsymbol{e}_0$ is the average number of primary knock-on atoms created at a depth $x$ from the surface and with energy $E_0$ into a solid angle $\boldsymbol{e}_0$, by an incident ion with initial energy $E_{inc}$ and direction $\boldsymbol{e}$: $P\mathrm{d}E_1\mathrm{d}^2\boldsymbol{e}_1$ is the probability that a recoil atom with ($E_0$, $\boldsymbol{e}_0$, $x$) is ejected from the surface with energy $E_1$ into a solid angle $\boldsymbol{e}_1$ without undergoing collisions. Atoms are ejected if they overcome the surface potential $U$. By assuming a planar barrier and considering the refraction at the surface, one has [4]

$$P(E_0,\boldsymbol{e}_0,x;E_1,\boldsymbol{e}_1)=\delta(E_1+U-E_0)\exp[-x/L\cos\theta_0]\delta(\varphi_1-\varphi_0)$$
$$\delta(\cos\theta_1-[(1+U/E_1)\cos^2\theta_0-U/E_1]^{1/2}), \qquad (13)$$

where $\theta_0$ and $\varphi_0$ are the polar angle and azimuth belonging to $\boldsymbol{e}_0$ with respect to the surface normal, whereas $\theta_1$ and $\varphi_1$ are the corresponding quantities belonging to $\boldsymbol{e}_1$: $\delta$ is the Dirac delta function: $L$ is the collision mean free path [4]. As discussed in Paper I, almost all light ions at near-normal incidence are subject to randomization because they are backscattered near $180^\circ$ by target atoms, and primary recoil atoms produced then by those ions are nearly isotropic [3,11]. Then we can assume $\hat{F}(E_{inc}, \boldsymbol{e}; E_0, \boldsymbol{e}_0, x) \approx \hat{F}(E_{inc}; E_0, x)/4\pi$. That almost all of the sputtered atoms are created near the surface is a fairy good approximation for sputtering of a heavy target material with light ions. Thus, we can also assume $\hat{F}(E_{inc}; E_0, x) \approx \hat{F}(E_{inc}; E_0, 0) \approx F_p(E_{inc}, E_0)$ in the integrand of eq.(12). Using eq.(13), one obtains for regions (I) and (II), respectively,

$$J(E_1,\boldsymbol{e}_1)=AL\cos\theta_1 E_1/\pi(E_1+U)^{9/4}\cdot[(\gamma(1-\gamma)E_{inc})^{1/4}-(E_1+U)^{1/4}], \qquad (14-\text{I})$$

$$J(E_1,\boldsymbol{e}_1)=BL\cos\theta_1 E_1/\pi(\gamma(1-\gamma))^{1/2}(E_1+U)^{5/2}$$
$$\cdot\ln[(B+E_{inc}{}^{1/2})/(B+(E_1+U)^{1/2}/(\gamma(1-\gamma))^{1/2})], \qquad (14-\text{II})$$

where $B = 2C_{1/2}(\gamma(1-\gamma))^{1/2}/K_L$. Integrating eq.(14) over $\boldsymbol{e}_1$ yields a differential sputtering yield in energy. We introduce a normalized energy distribution function of sputtered atoms, i.e., a normalized yield, $Y_N(E_{inc}, E_1)$, defined by a differential sputtering yield in energy divided by its sputtering yield. Then, $Y_N(E_{inc}, E_1)$ can be expressed for regions (I) and (II), respectively, as

$$Y_N(E_{inc},E_1)=N(E_{inc})E_1(E_1+U)^{-9/4}[(\gamma(1-\gamma)E_{inc})^{1/4}-(E_1+U)^{1/4}], \qquad (15-\text{I})$$

$$Y_N(E_{inc},E_1)=N(E_{inc})E_1(E_1+U)^{-5/2}$$
$$\cdot\ln[(B+E_{inc}{}^{1/2})/(B+(E_1+U)^{1/2}/(\gamma(1-\gamma))^{1/2})], \qquad (15-\text{II})$$

where $N(E_{inc})$ is a normalization factor. $N(E_{inc})$ is certainly dependent on a combination of projectile ion species and a target atom. It is noteworthy that the present formula (15) depends on incident ion energy $E_{inc}$.

## III. Results and discussions

We refer to sputtering yield data calculated with the ACAT code. In Figs. 1-3, we compare our results with the ACAT data for a Fe material irradiated normally by $D^+$ ions with incident energy of 50 eV, 100 eV and 1 keV. For these conditions, $T_l$ enters into region (II). Thus, we have used eq.(15-II) to calculate $Y_N(E_{inc}, E_l)$. Kenmotsu [3], Thompson [1] and Falcone [4] formulas are also referred to for comparison, where each spectrum is normalized to give a sputtered energy distribution function as discussed above. We have normalized the *truncated* Thompson formula (which includes a cut-off factor) and the conventionally used *untruncated* Thompson formula (which does not have a cut-off factor), by setting the maximum of sputtered energy at $\gamma E_{inc}$-$U$. Fig. 1 shows that our present formula and Kenmotsu's formula fit with the calculated data for 50 eV $D^+$ ions, although there is a difference between the data and our present formula at about $E_l$ = 0.5 eV. In contrast to these formulas, both Thompson formulas and the Faclone formula differ clearly from the ACAT data and have large tails even in the higher energy range where there are no ACAT data. In Fig. 2, our formula fits quite well with the ACAT data, and reasonable agreement is also seen for the Kenmotsu, Falcone and the *truncated* Thompson formulas. On the other hand, the *untruncated* Thompson formula differs clearly from the ACAT data and has again a large tail in the higher energy range. Fig. 3 shows that the peak value of the ACAT data differs from the present formula, the Falcone and the *untruncated* Thompson formulas by about 30 % for 1 keV $D^+$ ions. However, except for this discrepancy, they represent the spectrum well, whereas the Kenmotsu formula has a much smaller value at its maximum. Fig. 3 also shows that the *truncated* Thompson formula matches the ACAT data very well. In the 1-5 keV energy range of $D^+$ ions (not shown here), our present formula, the Falcone, and both Thompson formulas agree well with the ACAT data, except for the discrepancy at the peaks of the ACAT data.

## IV. Conclusions

To represent the energy distribution of atoms sputtered from a heavy material irradiated by light ions with a wide range of energy, we have extended a formula presented in Paper I, by considering inelastic and elastic energy losses and by keeping the same sputtering mechanism as before. However, we have assumed that primary knock-on atoms produced by backscattered ions do not lose energy while penetrating the material up to the surface, instead of the energy-loss model used in Paper I. We have expressed our formula in terms of a normalized energy distribution function and compared it with the ACAT data for 50 eV, 100 eV and 1 keV $D^+$ ions impinging on a Fe material. The agreement is very good for 100 eV. It is also good for 50 eV and 1 keV except for some differences near the peaks of the spectra. We have shown that there are considerable differences between the *truncated* Thompson formula and *untruncated* Thompson formula for 50eV and 100 eV. Our present formula agrees well with the ACAT data for incident light ions ($H^+$, $D^+$, $T^+$, $He^+$) with energy ranging from several tens of eV to about 2 keV and for heavy target materials, although the corresponding results have not been shown in this work.

**Acknowledgements**

The authors would like to thank Professor A.A. Haasz for making numerous corrections and for suggesting valuable changes. They also thank Professor H.J. Whitlow for his valuable comments. This work was supported partially by a Grant-in-Aid of the Academic Frontier Project promoted by the Ministry of Education, Culture, Sports, Science, and Technology of Japan. This work has been done under the collaboration research of National Institute of Fusion Science.

**References**


[1] M.W. Thompson, Philos. Mag. 18 (1968)377.

[2] H.L. Bay, B. Schweer, P. Bogen and E. Hint, J. Nucl. Mater. 111-112 (1982)732.

[3] T. Kenmotsu, Y. Yamamura, T. Ono, T. Kawamura, J. Plasma Fusion Res. Vol.80, No.5 (2004) 406-409.

[4] G.. Falcone, Surf. Sci. 187 (1987)212.

[5] Y. Yamamura, Y. Mizuno, IPPJ-AM-40, Inst. Plasma Physics Nagoya Univ. (1985).

[6] P. Sigmund, Rev. Roum. Phys. Tome 17, no. 8 (1972) 969.

[7] L. Lindhard, V. Nielsen, M. Scharff, K. Dan. Vidensk. Selsk. Mat-Fys. Medd. 36 no.10 (1968).

[8] S. Kalbitzer, H. Oetzmann, Radiat. Efft. 47 (1980)57.

[9] L. Lindhard, M. Scharff, Phys. Rev. 124 (1961)128.

[10] Y. Yamamura, J. Bohdansky, Vacuum 35 (1985)561.

[11] H.L Bay, J. Bohdansky, W.O. Hofer, J. Roth, Appl. Phys. 21 (1980)327.

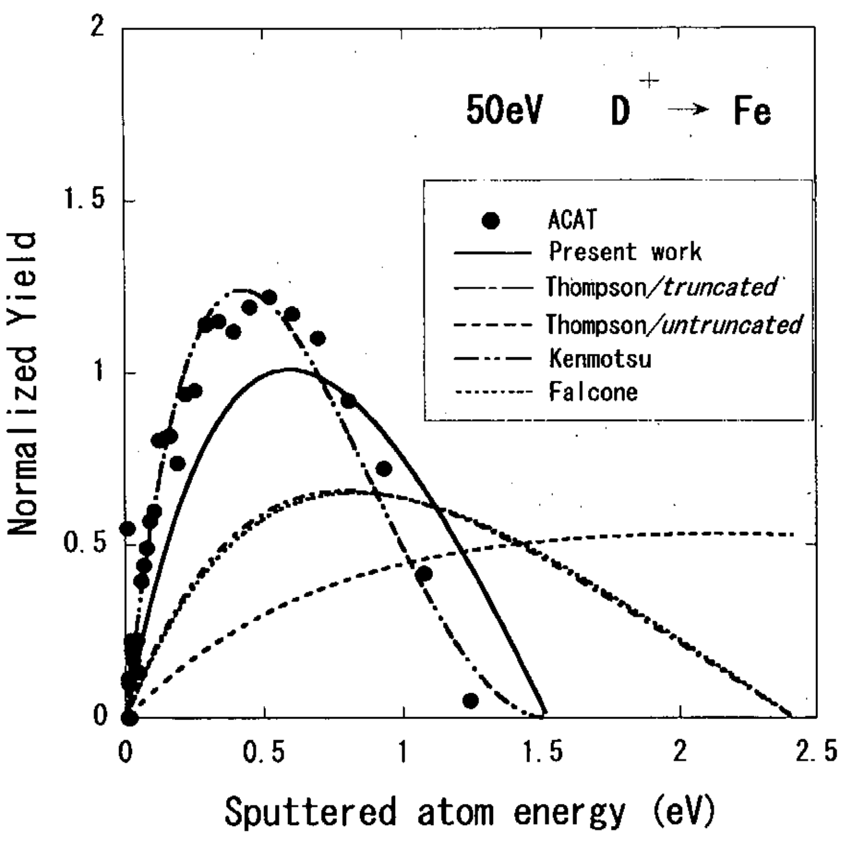


Fig.1 Normalized yields of atoms sputtered from a Fe material irradiated by 50 eV $D^+$ ions at normal incidence vs. sputtered atom energy in eV. The legend shows the curves obtained with the different formulas. The closed circles are the data calculated with the ACAT code. Note that the *truncated* Thompson and the Falcone curves completely overlap.

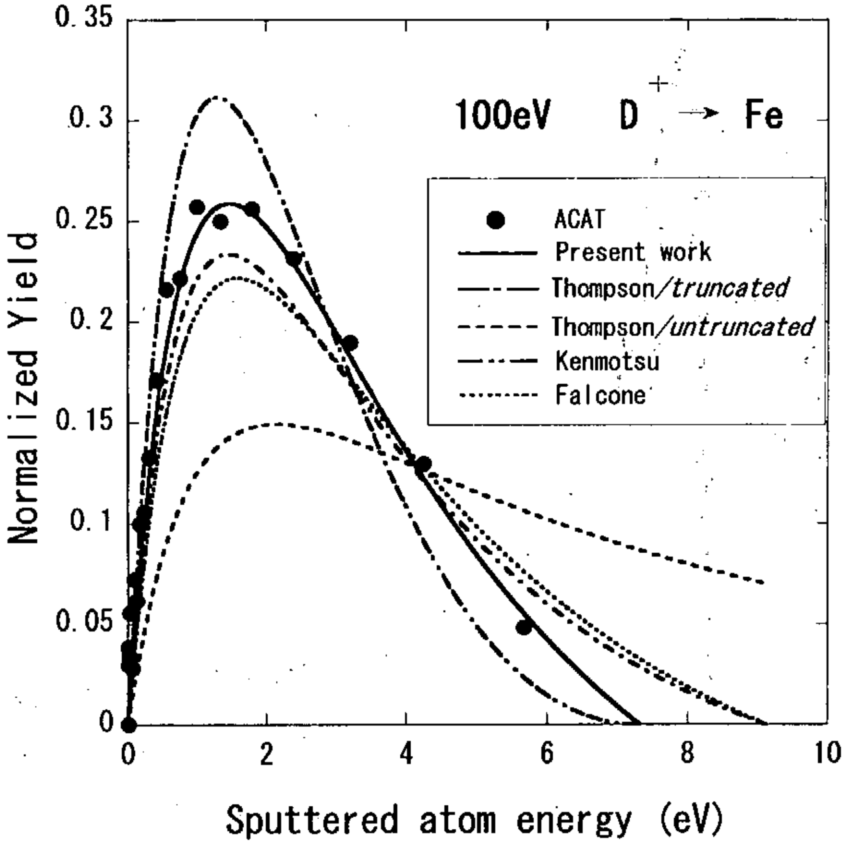


Fig.2 Normalized yields of atoms sputtered from a Fe material irradiated by 100 eV $D^+$ ions at normal incidence vs. sputtered atom energy in eV. Refer to Fig. 1 for legend.

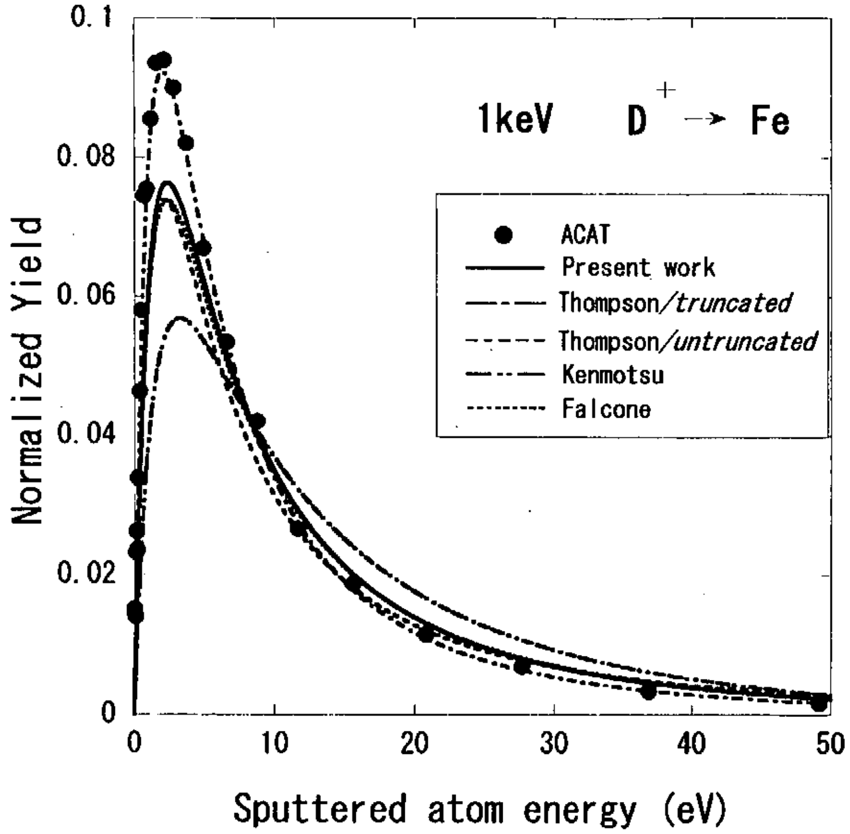


Fig.3 Normalized yields of atoms sputtered from a Fe material irradiated by 1 keV $D^+$ ions at normal incidence vs. sputtered atom energy in eV. Refer to Fig. 1 for legend.

# Publication List of NIFS-DATA Series

NIFS-DATA-72 M. Hayashi
Bibliography of Electron and Photon Cross Sections with Atoms and Molecules Published in the 20th Century – Argon –
Jan. 2003

NIFS-DATA-73 J. Horacek, K. Houfek, M. Cizek, I. Murakami and T. Kato
Rate Coefficients for Low-Energy Electron Dissociative Attachment to Molecular Hydrogen
Feb. 2003

NIFS-DATA-74 M. Hayashi
Bibliography of Electron and Photon Cross Sections with Atoms and Molecules Published in the 20th Century – Carbon Dioxide –
Apr. 2003

NIFS-DATA-75 X. Ma, H.P. Liu, Z.H. Yang, Y.D. Wang, X.M. Chen, Z.Y. Liu, I. Murakami and C. Namba
Cross-section Data Measured at Low Impact Energies for $Ar^{q+}$ Ions on Argon and Neon Targets
Apr. 2003

NIFS-DATA-76 M. Hayashi
Bibliography of Electron and Photon Cross Sections with Atoms and Molecules Published in the 20th Century – Sulphur Hexafluoride –
May 2003

NIFS-DATA-77 M. Hayashi
Bibliography of Electron and Photon Cross Sections with Atoms and Molecules Published in the 20th Century – Nitrogen Molecule –
June 2003

NIFS-DATA-78 A. Iwamae, T. Fujimoto, H. Zhang, D. P. Kilcrease, G. Csanak and K.A. Berrington
Population Alignment Collisional Radiative Model for Helium-like Carbon:
Polarization of Emission Lines and Anisotropy of the Electron Velocity Distribution Function in Plasmas
Aug. 2003

NIFS-DATA-79 M. Hayashi
Bibliography of Electron and Photon Cross Sections with Atoms and Molecules Published in the 20th Century – Xenon –
Sep. 2003

NIFS-DATA-80 M. Hayashi
Bibliography of Electron and Photon Cross Sections with Atoms and Molecules Published in the 20th Century – Halogen Molecules –
Dec. 2003

NIFS-DATA-81 M. Hayashi
Bibliography of Electron and Photon Cross Sections with Atoms and Molecules Published in the 20th Century – Water vapour –
Dec. 2003

NIFS-DATA-82 M. Hayashi
Bibliography of Electron and Photon Cross Sections with Atoms and Molecules Published in the 20th Century – Hydrogen molecules –
Feb. 2004

NIFS-DATA-83 M. Hayashi
Bibliography of Electron and Photon Cross Sections with Atoms and Molecules Published in the 20th Century - Hydrogen Halide Molecules -
Mar. 2004

NIFS-DATA-84 K. Ohya, A. Chen, J. Kawata, K. Nishimura, D. Kato, T. Tanabe and T. Kato
ELECTRAN - Monte Carlo Program of Secondary Electron Emission from Monoatomic Solids under the Impact of 0.1 - 10 keV Electrons
Mar. 2004

NIFS-DATA-85 I. Murakami, T. Kato, U.I. Safronova and A.A. Vasilyev
Dielectronic Recombination Rate Coefficients to Excited States of Boronlike Oxygen and Dielectronic Satellite Lines
May 2004

NIFS-DATA-86 I. Murakami , J. Yan , H. Sato , M. Kimura , R. K. Janev , T. Kato
Collision Processes of $Li^{3+}$ with Atomic Hydrogen: Cross Section Database
Aug. 2004

NIFS-DATA-87 M. Hayashi
Bibliography of Electron and Photon Cross Sections with Atoms and Molecules Published in the 20th Century - Ammonia and Phosphine -
Aug. 2004

NIFS-DATA-88 N. Yamamoto, T. Kato and F.B. Rosmej
Opacity Free and Space Resolved X-ray Diagnostics Based on Satellinte Lines near H-like Ly$\alpha$ of Highly Charged Ions
Sep. 2004

NIFS-DATA-89 T. Ono, Y. Aoki, T. Kawamura, T. Kenmotsu, Y. Yamamura
An Extended Formula for the Energy Spectrum of Sputtered Atoms form a Material Irradiated by Light Ions
Oct. 2004